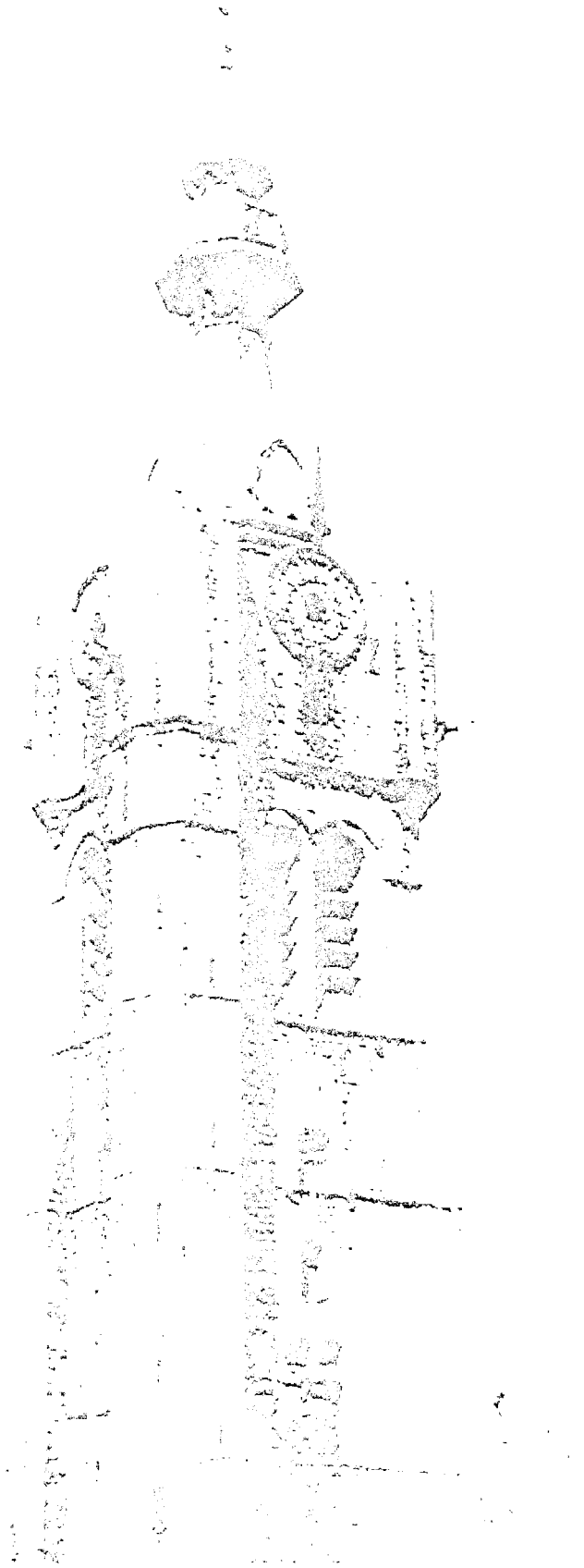

International
Seminar
on

VIBRATIONS AND ACOUSTIC NOISE OF ELECTRIC MACHINERY

[redacted]
25-26 May
1993

LABORATOIRE SYSTÈME [illegible]
[illegible]
[illegible]
FRANCE

INSTITUTE OF ELECTRIC MACHINES
AND TRANSFORMERS
TECHNICAL UNIVERSITY OF LODZ
POLAND

IMPACT OF INVERTER SUPPLY AND NUMERICAL CALCULATION TECHNIQUES IN AUDIBLE NOISE PROBLEMS

R.Belmans, K.Hameyer

Department Electrical Engineering-Division ESAT/ELEN
K.U.Leuven-Belgium
Kard.Mercierlaan 94
B-3001 Heverlee

1. INTRODUCTION

Audible noise in electromagnetic energy transducers is an electromechanical problem. In general two sources of audible noise exist in such devices: the magnetically generated noise, due to the magnetic forces in the magnetic circuit, and the airborne audible noise, due motion of the cooling air. Very typical for this problem is the fact that the overall behavior of the device under consideration is (efficiency, losses, power factor, heating, torque of rotating devices) is not influenced by the audible noise behavior.

Electrical machines and devices in general can exhibit vibrations that can generate audible noise when subjected to periodic forces caused by electromagnetic and aerodynamic sources. The fundamentals of the audible noise generation in induction motors will be discussed here. No mathematical details will be given, as they can be found in literature.

The topic of audible noise in induction motors goes back almost 80 years [1]. The aim of this review paper is not to present the full mathematical treatment, but rather to give insight in the physical phenomena governing the links between magnetics, mechanics and acoustics. Already in 1919, Stiel [1] has studied a four pole machine having rotors with different slot numbers. He showed that the audible noise level depends on the number of rotor slots Z_2. This indicates that the audible noise is not linked to the vibrations of the teeth. If this would be the case, it would be impossible to see how a minor change in number of rotor teeth (say + 1 or - 1 rotor slot) could have a major influence on the audible noise level. Also the tooth resonance do not have a significant role to play, certainly not in small and medium size motors. The longitudinal resonance frequencies are too high, while the bending resonances are too heavily damped. Stiel already gave a rule for the number of rotor teeth in which he indicated that odd rotor slot numbers have to be avoided. The work of Fritze [2]and Chapman [3] started a swift development. One tried to find rules for the magnetically caused audible noise in many different ways. Almost magically sounding rules were developed (use of prime numbers leading to relationship with respect to the divisibility), but also more physically based rules, aiming at a "good flux density distribution" [4]. The quality of the flux density wave was given by the voltage induced in a coil surrounding one stator tooth.

New rules for the slot numbers were given, that can be found in the important textbooks. A limited overview is given in Table 1 (e.g. [5-7]). Which rule is real, is not clear. The worst thing to do is to evaluate this rules statistically, although this has been done in the past.

Jordan [8] discusses the example of a 4 pole, 30 kW motor with 36 stator and 30 rotor slots. Due to the rules of Richter, this should have given a silent machine. In practice the motor was very noisy (825 Hz, 110 dB). In the analysis of Stiel, a motor with the slot combination 36/30 should be silent. One can wonder whether the slot combination has an influence whatsoever. Therefore, Jordan started a full study from scratch. He build a set of motors all 36 stator and 30 rotor slots, with rated power 5, 10, 15, 30, 100, 250 kW. The 5 and 10 kW were silent, the 15 kW could be noticed, 30 kW extremely noisy, and the 100 and 250 kW again silent. This points to the fact that the slot number combination and the dimensions of the motor are important for the audible noise.

The real problem is that not the slot combination as such is important, but that the magnetic and the mechanic design have to be considered together. Figure 1 shows the steps that lead to a correct prediction of the audible noise. We will now discuss some of the aspects more in detail in which we concentrate on the most important part: the magnetic noise [9,10].

The use of power electronics in various systems for power transformation, and especially in induction motors for controlling the speed, creates problems caused by the distortion of the supplied voltage and current. One such key problem is the higher audible noise level when compared to the motors supplied from the grid.

1	$N_2 + 2p \neq 6g+1$	Arnold-la Cour, Coers, Kron, Kade
2	$N_2 < N_1$	Heubach, Linker
3	$\frac{N_2}{p} = g$	Heubach, Linker
4	$N_2 = 2g$	Heubach, Linker, Möller, Kade
5	$\begin{cases} \lvert N_2 - N_1 \rvert \neq 1,3,5,\ldots \\ N_2 - N1 \neq 1, 2p \pm 1 \end{cases}$	Heubach, Raskop, Möller, Krondl Kron, Aperoff
6	$N_1, N_2 \neq g\,(6g+1)$	Linker
7	$N_1 - N_2 = p$, p even $N_1 - N_2 = 2p$, p odd	Linker
8	$N_2 \geq 2g$	Schulz
9	$N_2 = 2g+1$	Schulz
10	$N_2 = prime\ number * p \pm 1$	Raskop
11	$\lvert N_2 - N_1 \rvert \leq 10$	Raskop
12	$\frac{N_2}{2p} \neq 3g+1$	Dreese
13	$N_2 < 1{,}4\, N_1$	Krondl
14	$N_2 < 1{,}25\, N_1 + 2p$	Aperoff
15	$N_1 \neq N_2$	Arnold-la Cour, Rummel, Krondl, Aperoff
16	$\lvert N_1 - N_2 \rvert \neq p$	Kron, Aperoff
17	$\lvert N_1 - N_2 \rvert \neq 4p$	Aperoff

Table 1 Slot number rules

In addition, economic pressures force machine manufacturers to use less active material. Since the frame is less stiff, the machine becomes more sensitive to vibrations [11-13]. In addition, less iron is used in the stator, again yielding a weaker structure. Less iron also yields higher flux density values. At higher field levels, the forces causing the audible noise increase. Inverter supplied machines have been installed recently in environments requiring a quiet operation, as e.g. in air conditioning systems, printers, fans. Therefore, a far lower audible noise level is a prerequisite.

These constraints encourage the designer of electromagnetic systems toward the use of more advanced techniques to predict the audible noise. However, audible noise is a combined electromechanical problem, as first recognised by H.Jordan [8]. Electromagnetic forces cause the mechanical structure to vibrate. An example of an overall analysis including mechanical causes may be found in [14]. Most authors merely present either the mechanical [15,16] or the electromagnetic aspects [17-19] of the problem. In the last decade, the first analysis accounting for the influence of the inverters were published [20,21].

The overall analysis contains the steps, shown in figure 1. Clearly, this is a real electromagnetic-mechanic-acoustic problem. The last portion, the acoustic implications will not be treated here. Although magnetostriction in theory can contribute to the audible noise of rotating electric machines, its contribution in practice is negligible.

In this paper first attention is paid to the force calculations. Then the mechanical behavior is discussed. Last the combination of the motor with a speed control system is treated.

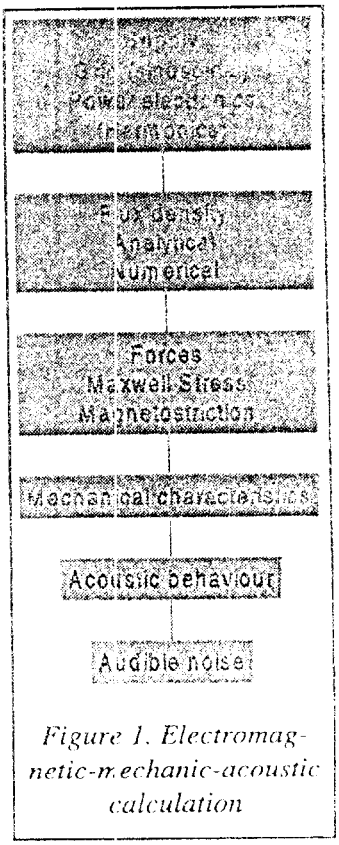

Figure 1. Electromagnetic-mechanic-acoustic calculation

2. FORCE CALCULATIONS: MAXWELL STRESS

At the surface of highly permeable ferromagnetic material, a force is generated that can be obtained from the Maxwell stress tensor. In electrical machines, the radial force at the teeth surface is:

$$\sigma = \frac{1}{\mu_0}\left[B_r^2 - \frac{1}{2}|B|^2\right] \tag{1}$$

Therefore, the accurate knowledge of the flux density distribution at the surface is recommended. Different methods exist to find this flux density distribution.

2.1 Rotating field theory

For electrical machines, and especially the induction motor, the best known technique is the rotating field theory. The flux density distribution is regarded as the superposition of an infinite number of flux density waves:

$$B_S(\alpha,t) = \sum_{\nu} \hat{B}_{S\nu} \cos\left(\nu\alpha - \omega_{\nu,k} t - \varphi_{\nu,k}\right) \tag{2}$$

When saturation and eccentricity are neglected, the space harmonic numbers for three phase machines are

$$\nu = (6g+1)p \qquad g = 0, \pm 1, \pm 2, \ldots \tag{3}$$

Corrections for saturation, eccentricity, slot harmonics are possible and may be found in literature. In general the flux density may be regarded as being perpendicular to the teeth surface, yielding a simplified representation of the Maxwell stress:

$$\sigma = \frac{B_S^2}{2\mu_0} \tag{4}$$

The pulsation $\omega_{V,k}$ in equation (2) is the supply pulsation or one of the harmonic components when the motor is inverter supplied. This leads to a number of traveling wave type forces all acting on the teeth. The analysis supplies the force components that act on the stator assembly. If the frequency of one of these force components interacts with one of the stator natural frequencies, resonance occurs and a high audible noise level may be expected. This way of thinking clearly indicates the importance of the sinusoidal voltage and current shapes in the supply: every harmonic leads to new force components, that may lead to audible noise components.

3. FINITE ELEMENT METHOD AND ACCURATE FORCE ASSESSMENT

To predict the forces that are important for the behavior of several classes of electromagnetic devices, the highest possible accuracy of the solution is required. Force and field quantities are derivatives from a potential formulation. The difficulty is due to the fact that the finite element method piecewise approximates the real potential by simple shape functions instead of obtaining the exact solution [22]. The accuracy of the solution depends on the

- type of discretization,
- choice of shape function and
- smoothness of the exact solution .

A lot of attempts based on the direct evaluation of the Maxwell stress as given by (1) or the virtual work principle have been made, but with limited success due to the explicit or implicit numerical differentiation encountered in each of them leading to a reduced accuracy. To surmount the loss in accuracy in a fundamental way, shape functions of higher order can be used. On the other hand, this would result in fast increasing computational expenses. A good trade-off between both considerations is the use of simple and fast linear shape functions and a local, accurate solution obtained by an analytical formulation, a potential interpolating function, yielding derived field quantities of the same order of accuracy as the potential solution. When analyzing electromagnetic devices often local values of the field quantities and the forces are of interest and therefore, the proposed local solution does not restrict the applicability of analysis.

For the local two-dimensional field problem, the basic idea is to determine the potential inside a circle analytically for given potentials applied as the boundary values at its circumference [23], [24]. The boundary values are supposed to be known from previous computations. This avoids the loss in order of convergence of the chosen approximation. Although other techniques could be used, the FEM is employed in the beforehand calculation. The boundary values of the local field problem are equally distributed along the circumference of a circle in 2D or a sphere in 3D. Then the field values at the center of the circle or the sphere are computed analytically.

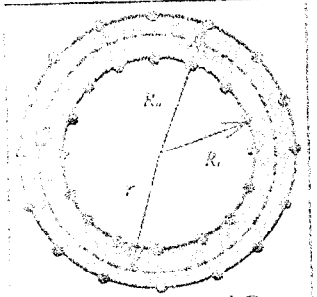

Figure. 2. Local DIRICHLET problem for a cylindrical air gap.

Starting from an existing FEM potential solution, the method describes a post-processor operator applied to the air gap region of an electromagnetic device. No restrictions concerning the finite element discretization are assumed. The proposed method is independent of the finite element mesh inside the domain. The results converge towards the values obtained by the classical evaluation of the potential solution using numerical derivatives if a very rough discretization or not suitable parameters are chosen e.g. the number of boundary potential values or the radius of the local field problem.

Another possible method uses the values of the magnetic vector potential on two concentric circles with radii R_i and R_O as boundary conditions (Figure 2). Local field values on the circular contour C with radius $R_i < r < R_o$ are calculated.

If the inner radius R_i is taken as a reference, the general solution of the LAPLACE's equation is

$$A_z(r,\Phi) = \sum_{k=1}^{N}\left(a_k\left(\frac{r}{R_i}\right)^k \cos(k\Phi) + b_k\left(\frac{r}{R_i}\right)^k \sin(k\Phi) + c_k\left(\frac{R_i}{r}\right)^k \cos(k\Phi) + d_k\left(\frac{R_i}{r}\right)^k \sin(k\Phi)\right) \tag{5}$$

The coefficients a_k, b_k, c_k and d_k are independently determined for each circular harmonic. Once the magnetic vector potential at the contour C is known, the normal and tangential component of the magnetic flux density can be determined:

$$B_n(r,\Phi) = \sum_{k=1}^{N}\left(-k\,a_k \frac{r^{k-1}}{R_i^k}\sin(k\Phi) + k\,b_k \frac{r^{k-1}}{R_i^k}\cos(k\Phi) - k\,c_k \frac{R_i^k}{r^{k+1}}\sin(k\Phi) + k\,d_k \frac{R_i^k}{r^{k+1}}\cos(k\Phi)\right) \tag{6a}$$

$$B_t(r,\Phi) = \sum_{k=1}^{N}\left(-k\,a_k \frac{r^{k-1}}{R_i^k}\cos(k\Phi) - k\,b_k \frac{r^{k-1}}{R_i^k}\sin(k\Phi) + k\,c_k \frac{R_i^k}{r^{k+1}}\cos(k\Phi) + k\,d_k \frac{R_i^k}{r^{k+1}}\sin(k\Phi)\right) \tag{6b}$$

The tangential force component F_t results in the torque T of the device. It can be shown [25,26] that the value of the torque is given by

$$T = \frac{2\pi}{\mu_0}\sum_{k=1}^{N}\left(k^2\left(b_k c_k - a_k d_k\right)\right) \tag{7}$$

being independent of the radius r of contour C. It is not necessary to calculate the normal and tangential component of the magnetic flux density on the contour, resulting in a faster algorithm, when the overall torque is recommended. The proposed method can be extended to time-harmonic problems. If all values are rms-values the torque is obtained by adding the torque calculated using the real- and the imaginary-component of the solution.

$$T = T_{real} + T_{imag} \tag{8}$$

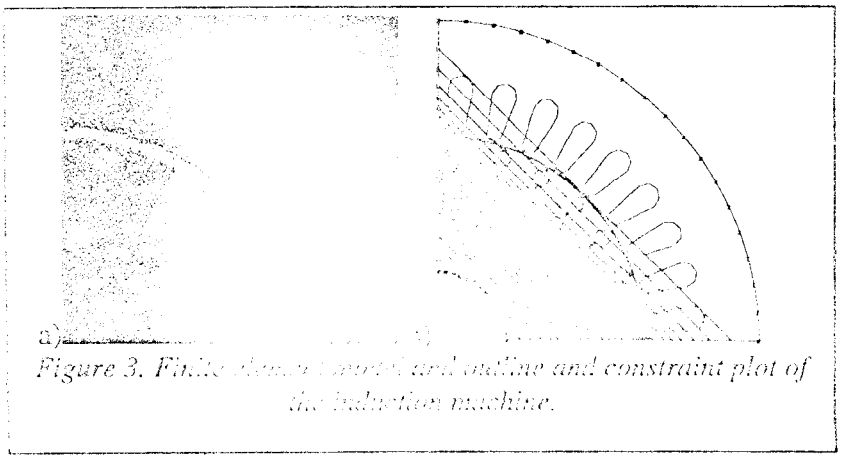

Figure 3. Finite element mesh and outline and constraint plot of the induction machine.

Figure 4 shows the variation of the torque for a varying radius r of the circular contour in the air gap of the induction machine. 1024 points are equidistantly distributed along the contour. The dashed line is the result applying the MAXWELL stress method classically. The first contour is placed in the middle of the first layer of elements in the air gap, the last one in the middle of the third layer. The solid line is the result of the LAPLACE based torque calculation. The result is symmetrical because two contours are needed to calculate the value of the resulting torque of the machine. Figure 4 shows that the conventional MAXWELL stress method strongly depends on the place of the contour inside the air gap, while the LAPLACE based method gives similar values for the torque as long as both contours are placed in the middle layer of elements. Furthermore, the conventional MAXWELL stress method is sensitive to the uniformity of the finite elements in the air gap.

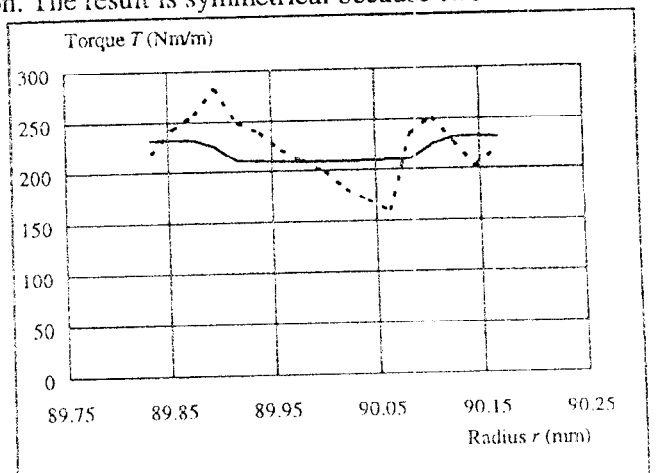

Figure. 4. Torque variation for different values of the radius r of circular contours C.

From this analysis it can be seen that force calculations based on the Maxwell stress method as the basis for the audible noise assessment of electrical machines have to performed with particular attention. It is far from evident that the classical rotating field theory yields worse results concerning the force distribution than the more advanced numerical solutions. Due to the numerical differentiation a lot of numerical noise may be introduced, yielding to in reality non existing audible noise components. The method described enhances the accuracy of derived field quantities i.e. field values and forces, derived from a potential solution. Results for local field values and forces point out their suitability.

4. MECHANICAL BEHAVIOUR

The electromagnetic forces lead to audible noise by exciting the mechanical structure. When looking at electrical machines, the Maxwell stresses at the surface of the stator are important. These forces essentially act on the top of the stator and rotor teeth. These teeth transfer the forces to the yoke, which passes the vibrations to the frame and the foundation. Therefore, it is important to see what parts of the machine are most susceptible to vibrations and thus contribute the most to the audible noise.

One could assume that the teeth vibrations would be the origin of the audible noise. However, a simple analysis shows this to be impossible. If this would be the case, a machine has to establish tones with a frequency being directly related to the number of stator teeth. This is in contradiction with the practical experience that the number of rotor slots clearly influence the audible noise behavior. However, one could assume that mechanical resonances of the stator teeth may be important. The teeth can only perform longitudinal vibrations, as bending is limited due to the damping effects caused by the winding. When such vibrations would be feasible, the acoustic path between the vibrations and the outside world would be very poor. When a tooth with parallel side surfaces is considered to be a beam, firmly connected to the yoke, with height h_T, the first natural frequency is:

$$f_{T=} = \frac{c}{4 \cdot h_T} \tag{9}$$

with the speed of sound in the ferromagnetic material being c=5260 m/s. For medium sized machines, the length is between 2 and 6 cm, yielding frequencies between 66 and 22 kHz, i.e. far beyond the audible noise spectrum. Therefore, no resonance can occur and only static loading has to be considered, leading to extremely small vibration magnitudes.

Therefore, the teeth merely act as a force transfer between the magnetic forces and the yoke. The yoke vibrations are the basis of the audible noise. In literature a massive number of papers have been presented all containing increasingly difficult analytical formulations for the natural frequency, trying to account for more and more detail. Jordan [8] and Tuteley [28] are probably the first authors to start this series. In his Ph.-D. Frohne [29] continues the work of Jordan and Verma [16] is probably the author that

went the deepest into the analytical formulations. Damping of the vibrations is generally neglected. Frohne shows that the winding adds to the damping, without changing the natural frequency. In recent years, this situation has changed. Due to the stiffer insulation material used (especially V.P.I. Vacuum Pressure Impregnation), the mechanical link between the conductors in the slot and the iron has become more stiff, and it is now better to represent the conductors as an extra mass.

Although this analytical formulation is very tentative, the calculation time involved in solving the equation system is large and may take several hours of computing time. Furthermore, it is essentially an analysis method, depending on the knowledge from experiments on existing systems, that are, in a certain way, extrapolated. It would, for instance, not be possible to extrapolate the results obtained from cylindrical machines, to machines with a square shaped lamination, as found in servomotors and new induction motor designs for inverter operated applications.

Apart from the principal disadvantages, the lack of technical detail is also a major drawback of the analytical methods. All of them assume the machine stator to be uniformly cylindrical. The effects of air-ducts spacers, the connecting box, the non-uniform stator core thickness and other regularities are neglected. The machine mounting significantly influences the natural frequencies and that also introduces asymmetries. The finite element method is capable of overcoming most of these problems [30].

ELIN 1,1 kW	Type LKM408M02F3B
U = 220/380 V	f = 50 Hz
I = 4,5/2,6 A	n = 2800 r/min
cos φ = 0,85	IP54
Insulation Class F	
24 stator slots	17 rotor slots

Table 2 Data of the induction motor used for experimental verification

Audible Noise peak [Hz]	Excitation [Hz]	Natural frequency [Hz] (measured)
364	fan	
524	532	500-540
424[2]	720	572
928	932	-
1208	1200	1198
1612[2]	1626	1736
1772	1760	1736
1936[2]	1920	1736
2176	2160	2280
2256[1]	2266	2280
2500[1]	2506	2576
2580	2586	2576
2740[1]	2719	2616

Table 3 Theoretical (column 2) and experimental (column 1) audible noise spectrum - nearest natural frequency is also given (column 3)

The finite element method has the following basic advantages:

- accurate representation of the stator iron cross-section, including the teeth;
- asymmetrical stator structure due to the airduct spacers, the non-uniform stator core thickness, the connecting box, the mounting and other irregularities may be accounted for;
- actual boundary conditions due to the machine mounting can be taken into consideration, being impossible in classical analysis techniques regarding the stator as being sus-

pended freely: it is evident that both eigenvalues and eigenmodes are influenced by the mounting.

Mode number	Frequency [Hz]
1	1122
2	1474
3	2515
4	2695
5	3468
6	4159
7	4930
8	5120
9	5552
10	6357

Table 4 Calculated natural frequencies of the 1,1 kW machine

The approach is used to calculate the natural frequencies of a 1.1 kW three phase squirrel cage induction motor with rated data given in Table 2.

The stator frame material is aluminium. Figure 5 represents the grid used and the most important modal shapes. In Table 4 the calculated natural frequencies between 1.000 and 6.500 Hz are shown.

The stator teeth are accounted for. As the elasticity modulus of copper is small with respect to the modulus of steel, the mass supplement due to the windings is more important than the supplementary stiffness introduced by it. However here both quantities are accounted for. The end windings are represented by masses added at the end of each slot. These adaptations to the model were necessary for the small motor as the influence of the windings on the natural frequencies is more important for lower machine ratings. The simple displacement geometries, as proposed in literature are not found in practice. This is particularly due to the influence of the machine mounting that becomes more important as the number of the eigenmode is higher. The experimental verification of the natural frequencies of a mechanical structure is generally performed using the modal analysis method. One of the experimentally recorded natural frequencies, 2.280 Hz, is not found in the theoretical study. This may be due to some of the irregularities not taken into account as e.g. the connecting box. Using more details in the analysis may resolve this problem. On the other hand, two theoretically found natural frequencies, 3.468 Hz and 4.930 Hz, are not in the experimental spectrum. This may be due to the fact that the accelerometer was mounted at a node of the model shape under investigation.

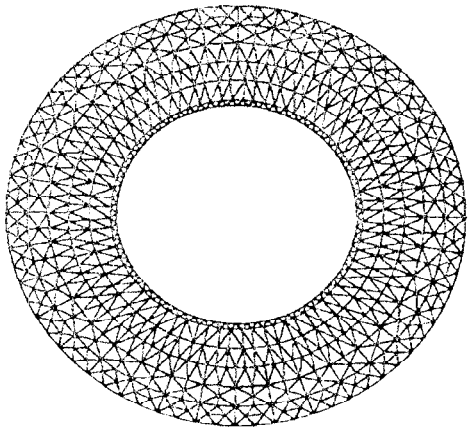

Mesh

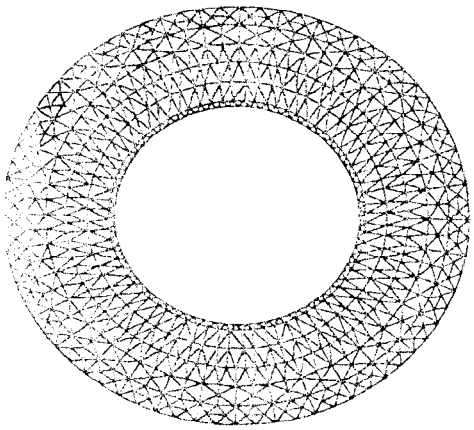

Second

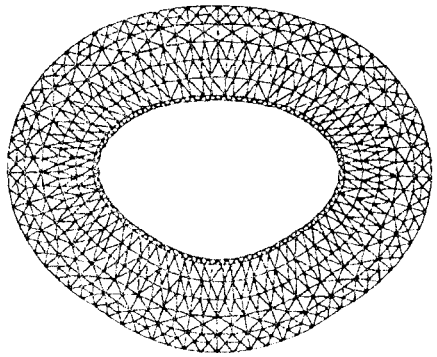

Third

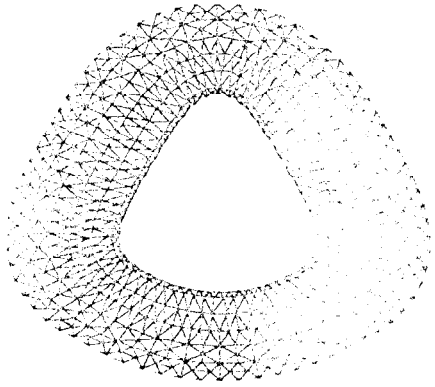

Fourth

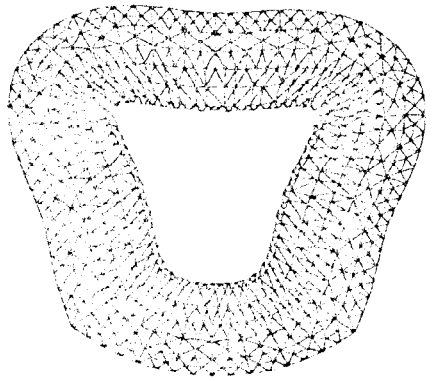

Sixth

Figure 5: Grid, second, third, fourth, and sixth eigenmode of the 1.1 kW induction motor (3D solution, 2D cut through the stator)

5. AUDIBLE NOISE OF INVERTER SUPPLIED INDUCTION MOTORS

Manufacturers claim that the increased switching frequencies lead to a low harmonic content reducing audible noise problems [31-36]. Due to the increased switching frequency, the harmonic content of the supplied voltages and currents is improved, leading to a diminished possibility of encountering resonance frequencies and thus high audible noise levels. This section describes a large number of experiments comparing audible noise in induction motor drives with different types of inverters and changing switching frequency.

5.1 Motor and inverter used

Tests are performed on different motor and inverter combinations (Figure 6). The first motor used is a standard 13.5 kW machine with a double cage rotor. The rated speed is 1455 rpm. The double bar construction is a standard design by European manufacturers. The rotor bars are skewed and made out of cast aluminium. These bars are not insulated with respect to the rotor iron leading to supplementary losses due to interbar currents. This type of rotor is required to increase the starting torque when supplying the motor directly from the mains (reference: SS motor, i.e. Standard stator; Standard rotor).

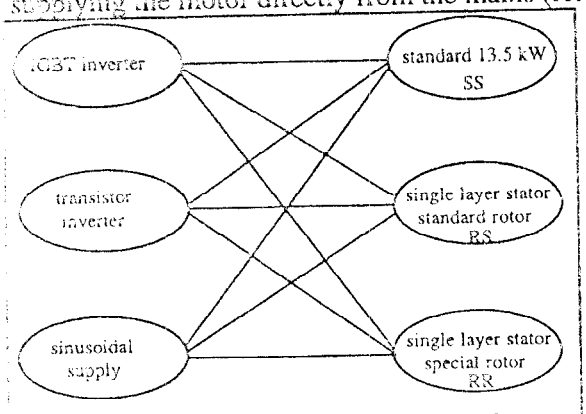

Figure 6: Different motor-supply combinations

In order to introduce temperature sensors in the stator, it is rewound. The original double layer winding is substituted by a single layer winding (RS motor: Rewound stator; Standard rotor).

In the double cage rotor current redistribution produces the high starting torque when the motor is connected to the mains. In inverter supplied induction motors, these starting problems are not present and current redistribution merely leads to an increase of the losses due to the harmonics of the non sinusoidal voltage. In order to assess the influence of current redistribution, a special rotor is built (RR motor, Rewound stator; Reconstructed rotor). This rotor has insulated round copper bars in open slots. The number of rotor bars is kept the same and no skewing is applied. The cross section area of the bars is chosen in a way that the dc resistance is equal to the original standard rotor. When mounted in the rewound stator, the motor is referred to as the RR motor.

Two types of inverters are used in the experiments. Both are voltage source inverters with Pulse Width Modulation (PWM). The first is transistor based and has a pre-set switching frequency. The second is an IGBT inverter with controllable switching frequency between 1 and 12 kHz. Unless otherwise mentioned, the tests are done in the normal operation mode, i.e. the Volts/Hertz ratio is kept constant. As a reference, all motors can be connected to a 50 Hz sinusoidal supply, since this yields the ultimate optimum regarding harmonic frequency content.

5.2 Measuring set-up

The induction motor is loaded with an eddy current brake that can be controlled accurately. The overall lay-out of the measuring set-up is shown on Figure 7.

The audible noise is measured in a semi-anechoic chamber, avoiding interference with the frequency inverter audible noise and reflections of the walls and other materials near to the set-up. The load has a very low audible noise level due to special bearings and water cooling. Both the overall noise levels in dB/in or dB(A), and its frequency spectrum are measured using a condenser microphone.

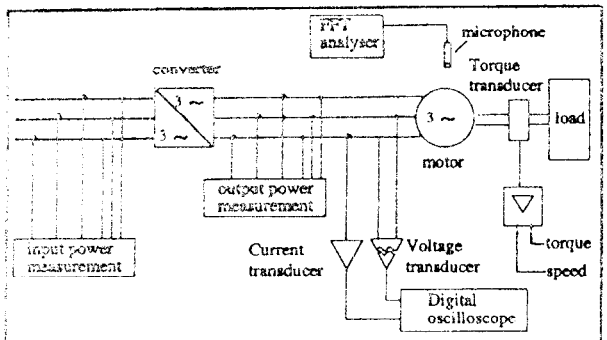

Figure 7: Lay-out of the experimental set-up

Even if the switching frequency can be controlled, as in the IGBT inverter, the inverter changes the operating switching frequency with respect to the pre-set and displayed value due to the internal logic circuit. Therefore, voltage and current spectra are monitored and recorded. From these spectra, the actual switching frequency can be determined. In tables and graphs below, the actual switching frequencies are provided.

5.3 Audible noise

5.3.1 Overall Audible Noise Level

The overall audible noise level is measured for each motor-supply combination at different loads. A selection of all the measurements is presented. As prescribed in the standards, a dB(A) filter is used. Table 4 shows the results at fundamental frequencies of 50 Hz and 30 Hz and a load torque of 60 Nm. The higher switching frequency reduces firmly the audible noise level. The difference relative to the mains supply is less than 1 dB(A). If a switching frequency of 1 kHz is used, (IGBT or transistor based inverter), the increase is more pronounced. The influence of switching frequency can be seen more clearly in figure 8, where the overall audible noise level at different fundamental frequencies is presented as a function of the switching frequency. The top graph shows the results for the standard motor (SS) loaded with 60 Nm torque and supplied by the IGBT inverter, while the bottom graph gives the results for the rewound stator with the original rotor (RS).

From these measurements, the following conclusions can be drawn.

TABLE 5 Audible noise [dB(A)] of different motor-supply combinations at a load of 60 Nm and fundamental frequency of 50 Hz (top) and 30 Hz (bottom)

Motor	Mains Supply Sinusoidal	IGBT-Inverter 1.2 kHz	IGBT-Inverter 12 kHz	Transistor Inverter 1 kHz
SS	74.8	78.0	75.5	77.0
RS	68.8	71.5	69.4	74.6
RR	75.1	77.0	75.4	77.7

Motor	IGBT-Inverter 1 kHz	IGBT-Inverter 12 kHz	Transistor Inverter 1 kHz
SS	75.2	69.6	75.0
RS	75.6	62.9	73.5

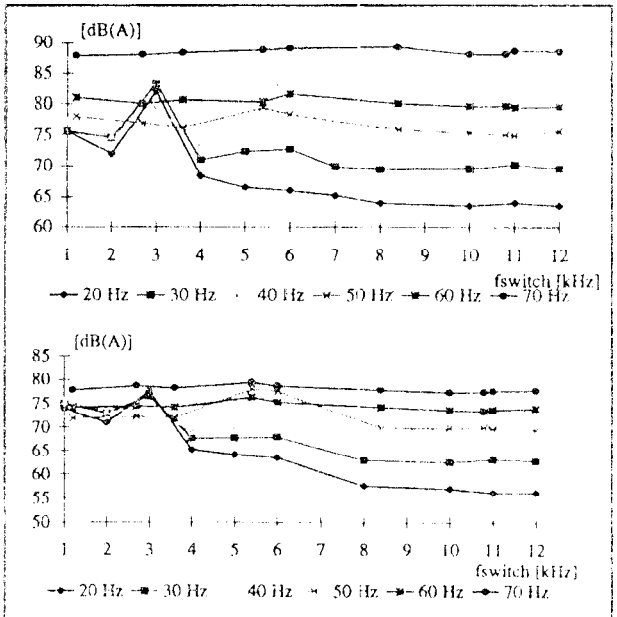

Figure 8: Overall audible noise level of standard motor (top) and single layer wound stator (bottom) as a function of the inverter switching frequency at different fundamental frequencies and a load torque of 60 Nm.

- At a switching frequency of 3 kHz, the overall audible noise level is higher than expected in the case of fundamental frequencies up to 40 Hz. This is due to the excitation of a natural frequency of the stator by the frequency of one of the vibrations produced by the electromagnetic forces caused by the switching frequency. For the motor with double layer stator winding at higher frequencies these phenomena do not occur.

- In the case of the modified stator, a higher level is also recognised at 50 Hz (f_{switch}= 5.4 -6 kHz) and at 40 Hz (f_{switch}= 11 kHz). This is due to the occurrence of subharmonics in the voltage spectrum, as noticed in figure 11.
- Generally the overall audible noise level decreases when the switching frequency increases. Particularly up to 8 kHz and fundamental frequencies below 50 Hz, there is a large drop in the audible noise. Thus, at lower motor speeds the overall audible noise is strongly reduced by applying higher switching frequencies. Once the switching frequency is above 8 kHz, the overall audible noise level is stabilized.
- At higher fundamental frequencies respectively at higher motor speeds the overall audible noise level has a small decrease as the switching frequency increases: the audible noise of the fan dominates the overall audible noise level.
- If no resonance occurs between the forces caused by the space harmonics in the flux density distribution in the air gap, and the stator natural frequencies, the motor with the single layer stator winding produces less audible noise than the original motor. This is due to the more stiff type of insulation material used during rewinding: a higher class of insulation material is used, generally leading to a higher stiffness of the link between stator winding and stator iron as indicated by Verdyck et al [35,36].
- Considering the motor with the copper rotor, it can be stated that the audible noise level is higher than using the original rotor (Table 5), caused by the high number of slotting harmonics. The harmonics are due to the fact that the new rotor has open rotor slots, while the original one has closed ones. Furthermore, the copper rotor is not skewed, again increasing the influence of the harmonics, and thus increasing the audible noise level.

5.3.2 Audible Noise Spectrum

All measurements are performed in dB without filtering the input signal of the microphone. Apart from the level as such, single tones may be noticed in the spectra.

In order to show the influence of the frequency spectrum of the supplied voltage, the spectra of the audible noise are compared. As an example, figure 9 shows the frequency spectrum of the RS motor loaded with 75 Nm when supplied consecutively from the 50 Hz mains and the transistor inverter. In the inverter supply spectrum, a large number of single tones are present. The high peak of 71 dB at about 1.1 kHz is caused by one of the sidebands in the voltage spectrum. Figure 10 shows the audible noise spectrum of the same motor at the same speed and load conditions, but supplied by the IGBT-inverter switching at 12 kHz. Thus, one could conclude that the frequency spectrum at high switching frequencies is improved a lot.

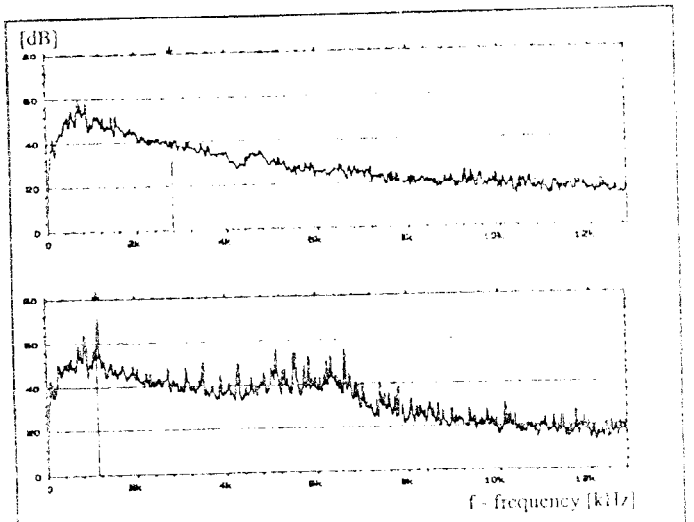

Figure 9: Audible noise spectrum of RS motor with 50 Hz sinusoidal and 50 Hz transistor inverter supply (switching frequency 1 kHz)

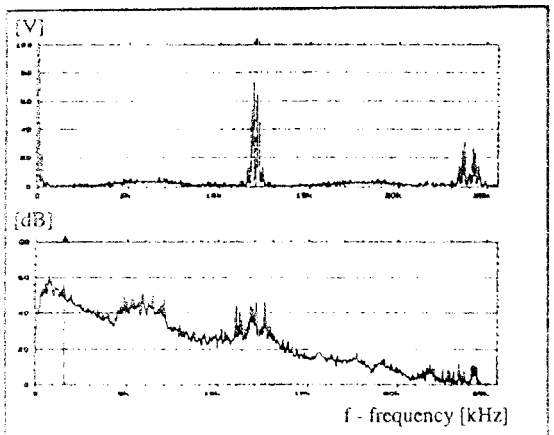

Figure 10: Voltage and audible noise spectrum of RS motor with IGBT-inverter supply (12 kHz)

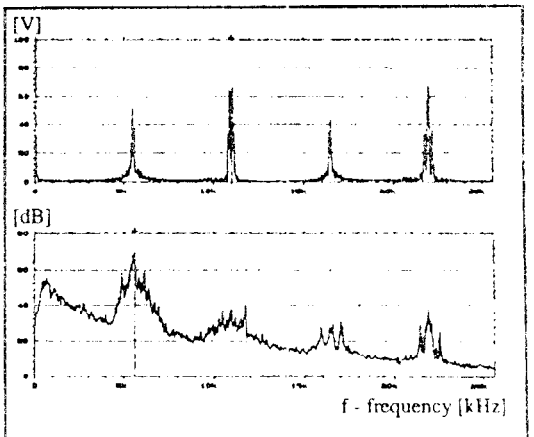

Figure 11: Voltage and audible noise spectrum of RS motor with IGBT-inverter supply (11 kHz)

In some cases, however, strong subharmonics appear causing more single tones. Figure 11 shows the voltage and noise spectrum for the same motor at a fundamental frequency of 40 Hz and a switching frequency of 11 kHz. Also the overall noise level increases, as noticed above (figure 8). As the human ear is particularly sensitive to single tones, the audible noise of inverter supplied machines containing such tones is found to be very disturbing. This problem may be cured by using random PWM techniques: rather than avoiding an increase of the overall level, they reduce the presence of audible noise components having single tones. Sometimes the high switching frequencies are not the best choice due to the increase of the inverter losses, being partially proportional to the number of switching instants per unit time, i.e. the switching frequency. Therefore, a lower frequency is used combined with a slightly varying pulse pattern. This approach avoids resonances and thus the appearance of single tones in the spectrum. As the human ear is very susceptible to such single tones, the use of this technique leads to a better accepted audible noise. However, the overall dB(A) values, often used when ordering drives, is higher. Therefore, the results of the study indicate the importance of a correct definition of the audible noise quality of a drive, that can definitely not be limited to one simple dB(A) figure.

6. CONCLUSIONS

The mechanical characteristics of the magnetic circuit is very important with respect to the audible noise behavior of electromagnetic energy transducers. The magnetic forces excite the mechanical structure, especially when resonance occurs, large vibration magnitudes and thus high audible noise levels may be expected. Two type of forces are important: Maxwell stress and magnetostriction. It is shown that magnetostriction plays a limited role in the audible noise of induction motors, but can contribute to the audible noise of other devices, machines, transformers, inductors, in a noticeable way. The analysis methods, numerically and analytically, that can be used to calculate the magnetic field, the forces and the mechanical behavior are given, with special emphasis towards the pitfalls that may be encountered, giving ways to come around them. In the last portion, the importance of the inverter supply, becoming increasingly important in practice for controlling the speed of induction motors with the aim of energy conservation, is given. It is shown how the high switching frequencies contribute to a significant reduction of the audible noise level.

7. ACKNOWLEDGEMENTS

The authors are indebted to the Belgian "Nationaal Fonds voor Wetenschappelijk Onderzoek" for its financial support for this work and the Belgian Ministry of Scientific Research for granting the IUAP No.P4/20 on Magnetic Fields.

8. REFERENCES

[1] Siel W.: "Experimentelle Untersuchung der Drehmomentverhältnisse mit Kurzschlußrotoren verschiedener Stabzahl," Forschungsarbeiten auf dem Gebiete des Ingenieurwesens, Heft 212, 1919.

[2] Fritze H.: "Über die Geräuschbildung bei elektrischen Maschinen," Arch.Elektrotechn. Bd.10, 1921, pp.73.

[3] Chapman F.T.: "The production of noise and vibrations by certain squirrel-cage induction motors", J.A.I.E.E., Vol.61, 1922, pp.39.

[4] Riggenbach M.: "Die Geräuschbildung der Induktionsmotoren," BBC-Mitt.20, 1933, pp.126-130.

[5] Krondl M.: "Die parasitären Kräfte in Induktionsmaschinen," Bull.Oerlikon 24, 1931, pp. 654, 625, and pp.665-670.

[6] Kron G.: "Induction motor slot combinations," Electr.Engg., Vol.50, 1931, pp.757.

[7] Möller H.: "Über die Drehmomente beim Anlauf von Drehstrommotoren mit Käfiganker," Arch. für Elektrotechnik, Bd.24, 1930, pp.401-424.

[8] Jordan H.: "Der geräuscharme Elektromotor," Verlag W.Girardet, Essen, 1950.

[9] Frohne H., Jordan H.: "Augenblicklicher Stand der Lärmbekämpfung bei Drehstromasynchronmotoren," Lärmbekämpfung, 1958, pp.27-31.

[10] Frohne H.: "Über die primären Bestimmungsgrößen der Lautstärke bei Asynchronmaschinen," Ph.D. TH Hannover, 1959.

[11] Verdyck D., Belmans R., Geysen W.: "An acoustic model for a permanent magnet machine: modal shapes and magnetic forces," IEEE Industry Applications Society Annual Meeting, Houston, Texax, USA, October 4-9, 1992, pp.292-299.

[12] Belmans R., Geysen W., Verdyck D.: "The use of the stator's modal shapes in the calculation of its vibrations," International Workshop on Electric and Magnetic Fields, Liège, 28-30 September 1992, pp.66.1-66.6.

[13] Verdyck D., Belmans R., Geysen W.: "A model for the induced mechanical vibrations in the stator of an inverter fed electrical machine," 17th International Seminar on Modal Analysis, K.U.Leuven, pp.871-885.

[14] Belmans R., Geysen W., Tuinman E., Gordens J.C.A.M.: "Vibration aspects of the design of a new generations of dc motors for the propulsion of submarines," IEEE Industry Applications Society Annual Meeting, Houston, Texas, October, 1992, pp.79-85.

[15] Staiger A., Jordan H.: "Der Einfluß des Gehäuses auf das Schwingungstechnische Verhalten des Ständers von Drehstrommaschinen," AEG Mitteilungen (1962), pp.194-202.

[16] Verma S.P., Girgis R.S.: Resonance frequencies of electrical machines stators having encased construction Part I and II," IEEE, Vol.PAS-92, 1973, pp.1577-1593.

[17] Ellison A.J., Moore C.J.: "Acoustic noise and vibrations of rotating electrical machines," Proc.IEE, Vol.115 (1968), pp.1633-1640.

[18] Tsivitse P.J., Weihsmann: "Polyphase induction motor noise," IEEE, Trans.Ind.Gen.Appl., Vol.IGA-7, May/June, 1971, pp.339-359.

[19] Landy C.F.: "An investigation into some aspects of noise and vibration produced in rotating electric machines," Transactions SA Inst. Elec. Eng., Sept. 1975, pp.190-197.

[20] Gießler F., Sattler Ph.-K.: "Magnetic noise of induction machines by inverter suplly," Proceedings International Conference on Electrical Machines, ICEM-88, Pisa (Italy), September 1988, pp.611-616.

[21] Gießler F.: "Asynchronmaschinen mit konventionellen und Wärmerohrkühlung am U- und I-Umrichter, Vergleich der Ausnutzung, der Verluste und der Geräusche," Ph.-D., R.W.T.H.-Aachen, Germany, 1988.

[22] Zienkiewicz, O.C. and Taylor, R.L.: The Finite Element Method, 4th edition, Vol. 1: Basic formulation and linear problems, McGraw-Hill Book Company, 1994.

[23] Kasper, M. and Franz, J., "Highly accurate computation of field quantities and forces by superconvergence in finite elements", IEEE Trans. on Magnetics, 1995, Vol. 31, No. 3, pp. 1424-1427.

[24] Meis, Th. and Marcowitz, U., Numerical Solution of Partial Differential Equations, Appl. Math. Science 32, Springer Verlag, 1981.

[25] Mertens, R., DeWeerdt, R., Pahner, U., Hameyer, K. and Belmans, R., "Force calculation based on a local solution of Laplace's equation", proc. 7th Biennial IEEE Conference on Electromagnetic Field Computation, CEFC'96, Okayama, Japan, March 19-20, 1996, p. 354.

[26] Salon, S.J., Finite element analysis of electrical machines, Kluwer Academic Publisher, Boston, London, Dordrecht, 1995.

[27] De Weerdt, R., Hameyer, K., Belmans, R., "End winding leakage calculation of a squirrel-cage induction motor for different load conditions", International Journal for computation and mathematics in electrical & electronic engineering (COMPEL), vol.14, no.4, Dec. 1995, pp.85-88.

[28] Erdely E.: "Predetermination of Sound Pressure Levels of Magnetic Noise of Polyphase Induction Motors," Transactions of the AIEE, December 1955

[29] Frohne H.: "Über die primären Bestimmungsgrößen der Lautstärke bei Asynchronmaschinen," Ph.-D. T.H.Hannover, July 1959

[30] R.Belmans, P.Cornelissen, A.Vandenput, W.Geysen: "CAD-Finite element combination for calculating natural frequencies of machine stators," International Conference on Evolution and Modern Aspects of Induction Conference, July 8-11, 1986, Turino, Italy.

[31] A.Malfait, R.Reekmans, R.Belmans: "Audible noise and losses in variable speed induction motor drives with IGBT inverters-Influence of the squirrel cage design and the switching frequency" 29th Annual Meeting IEEE-IAS, Denver-Colorado, USA, 2-6 Oct.. 1994, Vol.I-pp.693-700.

[32] Belmans R., Verdyck D., Geysen W., Findlay R.: "Electromechanical analysis of the audible noise of an inverter-fed squirrel-cage induction motor," IEEE Transactions on Industry Applications, Vol.27, No.3, May/June 1991, pp.539-544.

[33] Belmans R., Geysen W., Bailly G., Sattler P-K.: "Theoretical and experimental analysis of the audible noise of an inverter fed squirrel cage induction motor," International Conference on Electrical Machines ICEM-90, Cambridge, Massachusetts, U.S.A., August 13-15, 1990, pp.485-490.

[34] J.Muster, P.K.Budig, R.Belmans, W.Geysen: "Audible noise in speed-controlled inverter-fed medium-sized induction motors", ETEP, Eurel publication, vol.5, no.1, Jan/Febr.1995, pp.5-13.

[35] D.Verdyck, R.Belmans: "A vibrational model using modal shapes and magnetic forces: experimental results for a permanent magnet machine," Archiv für Elektrotechnik 77, 1994, pp.383-389.

[36] D.Verdyck, R.Belmans: "An acoustic model for a permanent magnet machine: Modal shapes and magnetic forces", IEEE Transactions on industry applications, Nov./Dec.1994, vol.30, no.6, pp.1625-1631.